Quantum and semiclassical inelastic electron transport

Kelly C. Magruder*
Department of Electrical Engineering, University of Southern California, Los Angeles, California 90089-2533, USA

A. F. J. Levi
Department of Physics and Astronomy, University of Southern California, Los Angeles, California 90089-0484, USA
and Department of Electrical Engineering, University of Southern California, Los Angeles, California 90089-2533, USA
(Received 18 March 2010; published 9 June 2010)

Quantum-mechanical calculation of coherent electron transmission in the presence of inelastic electron-phonon interaction is calculated and compared with the semiclassical predictions of simple first-order perturbation theory. It is found that a small electron-phonon matrix element cannot be used to justify semiclassical behavior. Only if the transmission coefficient is small enough at the phonon threshold, causing unitary feedback effects to occur primarily in reflection, do nonperturbative and first-order perturbative solutions appear qualitatively similar. There are situations in which predictions of simple perturbation theory cannot approach the nonperturbative quantum calculation even in the presence of both weak coupling and large elastic-scattering strengths.

DOI: 10.1103/PhysRevB.81.235312 PACS number(s): 73.40.Gk, 03.65.Nk, 72.10.Di, 73.50.Bk

I. INTRODUCTION

Inelastic electron scattering can play a critical role in determining the transport properties and performance of electron devices. Typically, processes such as electron-phonon scattering are treated as incoherent events and the scattering rates are calculated using simple first-order time-dependent perturbation theory. This approach ignores unitarity and coherent processes that could exist and be important in small nanoscale devices. Simple first-order perturbative approximations cannot access key features of nonperturbative quantum predictions. The preservation of unitarity in a self-consistent quantum model drives a feedback mechanism between all inelastic channels. Even under the condition of weak coupling, which is commonly invoked to justify perturbation theory, the incident electron must be affected by the existence of inelastic channels and there is no guarantee that the predictions of first-order perturbation theory can qualitatively mimic the behavior of a nonperturbative quantum model.

Nonequilibrium Green's functions (NEGFs) can be used to incorporate many-body effects[1] into the Landauer model of electron transmission.[2,3] However, these many-particle interactions make numerical solutions to the NEGFs intractable and usually force one to resort to first-order perturbative methods. This often reduces the solution to a random-phase approximation, averaging out many quantum-mechanical effects and resulting in a semiclassical approximation often interpreted in terms of tunneling and scattering rates for localized particles.

To solve the inelastic-scattering problem nonperturbatively we use an established prototype model[4–7] that considers the interaction between an electron and a localized vibrational mode (an Einstein phonon). This model has been used to investigate feedback-related features such as Fano-like resonances in the transmission,[8] impurity band formation in quantum wells,[9] and inelastic effects on wave-packet propagation.[10] The model has a very rich solution space which may be attributed to treatment of the electron-phonon interaction as a coherent and unitary process even though it does not include many-body and some self-consistent effects such as energy level shifts, collisional broadening, and electron-electron interactions. In the following, we assume it is more important that an exact solution be obtained to a simpler model than a perturbative solution be obtained to a more complex model, such as in Ref. 11.

II. THEORY

Inelastic scattering between an electron and dispersionless phonons is modeled by Einstein phonons linearly coupled to the electron wave function. We consider one-dimensional electron transport in the x direction in a semiconductor. It is assumed that the electron density is sufficiently small that electron-electron interactions may be ignored. For an electron of effective mass m interacting with Einstein phonons, the Hamiltonian is[4]

$$\hat{H} = -\frac{\hbar^2}{2m}\frac{\partial^2}{\partial x^2} + V(x) + \hbar\omega_0 \hat{b}^\dagger \hat{b} + g_1(\hat{b}^\dagger + \hat{b})\delta(x - x_0), \quad (1)$$

where the first two terms are kinetic energy and potential energy of the electron, respectively; the third term is the total energy stored in the phonons; and the final term couples the electron to the Einstein phonons located at position $x=x_0$. The creation and annihilation operators for a phonon of energy $\hbar\omega_0$ are $\hat{b}^\dagger$ and $\hat{b}$, respectively. The electron-phonon coupling constant is g_1 and has units of energy times distance. We assume that a conduction-band electron interacts with a longitudinal-optic (LO) phonon via the Frölich interaction in the semiconductor GaAs at temperature $T=0$ K. The effective electron mass is $m=0.07m_0$, where m_0 is the bare electron mass, and the phonon energy is $\hbar\omega_0 = 36$ meV.

When the electron inelastically scatters it may lose (gain) energy by emitting (absorbing) a phonon. The number of phonons excited by the electron is n, with positive n denot-

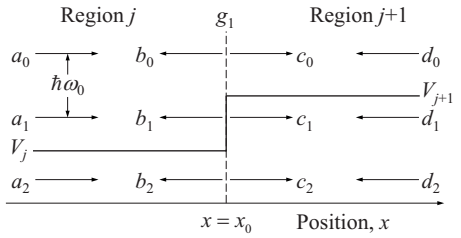

FIG. 1. Diagram of a potential step with Einstein phonons located at position $x=x_0$. Electron waves are incident from the left and right with amplitudes a_n and d_n, respectively. Waves will be scattered from position $x=x_0$ to the left and to the right having amplitudes b_n and c_n, respectively. The electron-phonon coupling constant is g_1 and the phonon energy is $\hbar\omega_0$.

ing a net emission of phonons. Conservation of energy requires that the electron's final energy be $E_n=E_0-n\hbar\omega_0$, where E_0 is the injection energy of the electron. The existence of a ground state restricts $n\geq 0$.

The propagation matrix method[12,13] may be used to solve the Schrödinger equation for states,

$$\Psi_k(x) = \sum_n \psi_{k,n}(x)|n\rangle. \tag{2}$$

Here, it is assumed that the electron, ψ, and phonon, $|n\rangle$, wave functions are separable. The domain of interest is discretized in space and the static potential $V(x)$ is approximated as a series of potential steps. The diagram in Fig. 1 shows two regions of the domain separated by a potential step and Einstein phonons located at position $x=x_0$. The electron states in regions j and $j+1$ are assumed to be of the form

$$\psi_{k,n}(x) = a_n e^{ik_n^j x} + b_n e^{-ik_n^j x}, \tag{3}$$

for $x\leq x_0$, and

$$\psi_{k,n}(x) = c_n e^{ik_n^{j+1} x} + d_n e^{-ik_n^{j+1} x}, \tag{4}$$

for $x\geq x_0$, where

$$k_n^j = \frac{\sqrt{2m(E_n - V_j)}}{\hbar}. \tag{5}$$

The Schrödinger equation is solved by first integrating about position $x=x_0$ to give

$$\left.\frac{\partial\psi_n}{\partial x}\right|_{x=x_0^+} - \left.\frac{\partial\psi_n}{\partial x}\right|_{x=x_0^-} = \sqrt{n}\frac{2mg_1}{\hbar^2}(c_{n-1}+d_{n-1}) + \sqrt{n+1}\frac{2mg_1}{\hbar^2}(c_{n+1}+d_{n+1}). \tag{6}$$

Substituting Eqs. (3) and (4) into Eq. (6) and forcing continuity of the wave function yields the recursion relations

$$a_n = i\sqrt{n}\frac{mg_1}{\hbar^2 k_n^j}(c_{n-1}+d_{n-1}) + \frac{1}{2}\left(1+\frac{k_n^{j+1}}{k_n^j}\right)c_n + \frac{1}{2}\left(1-\frac{k_n^{j+1}}{k_n^j}\right)d_n + i\sqrt{n+1}\frac{mg_1}{\hbar^2 k_n^j}(c_{n+1}+d_{n+1}), \tag{7}$$

$$b_n = -i\sqrt{n}\frac{mg_1}{\hbar^2 k_n^j}(c_{n-1}+d_{n-1}) + \frac{1}{2}\left(1-\frac{k_n^{j+1}}{k_n^j}\right)c_n + \frac{1}{2}\left(1+\frac{k_n^{j+1}}{k_n^j}\right)d_n - i\sqrt{n+1}\frac{mg_1}{\hbar^2 k_n^j}(c_{n+1}+d_{n+1}), \tag{8}$$

which allow each channel n to feed into channel $n+1$ and feed back into channel $n-1$.

We solve for the electron wave function at the left and right edges of the system by creating propagation matrices $\mathbf{P}_j$ for each region of the domain and solving

$$\begin{bmatrix} a_0 \\ b_0 \\ \vdots \\ a_N \\ b_N \end{bmatrix} = \prod_j \mathbf{P}_j \begin{bmatrix} c_0 \\ d_0 \\ \vdots \\ c_N \\ d_N \end{bmatrix}, \tag{9}$$

where N inelastic channels are included in the simulation and each of a_n and d_n is given by boundary conditions.

The inelastic channels are independent due to the orthogonality of the oscillator states $|n\rangle$. The total electron transmission is then the sum of the transmission probabilities of all propagating channels,

$$T(E_0) = \sum_{n=0}^{E_0/\hbar\omega_0 - 1} T_n(E_0) = \sum_{n=0}^{E_0/\hbar\omega_0 - 1} \frac{k_n}{k_0}|c_n(E_0)|^2, \tag{10}$$

where the upper limit of the summation ensures that only propagating modes contribute and the velocity normalization ensures unitarity.

A. Strong-coupling regime

Numerical solutions require that only a finite number of phonons are included in the simulation. However, the solution to the truncated system will not converge with increasing N when g_1 exceeds a critical value $g_{1,c}$. For $g_1 > g_{1,c}$, the inelastic channels are so strongly coupled that all inelastic channels contribute significantly to the total response of the system, and hence the matrix may not be truncated for any value of N.

To determine $g_{1,c}$ analytically consider the continued fraction solution,

$$c_0 = \cfrac{1}{1 + \cfrac{\frac{m^2 g_1^2}{\hbar^4 k_0 k_1}}{1 + \cfrac{\frac{2m^2 g_1^2}{\hbar^4 k_1 k_2}}{1 + \ddots}}}. \tag{11}$$

For large N the coupling element approaches

$$\lim_{N\to\infty} i\frac{\sqrt{N}mg_1}{\hbar^2 k_N} = \frac{\sqrt{mg_1}}{\hbar\sqrt{2\hbar\omega_0}}, \tag{12}$$

and the continued fraction expansion becomes

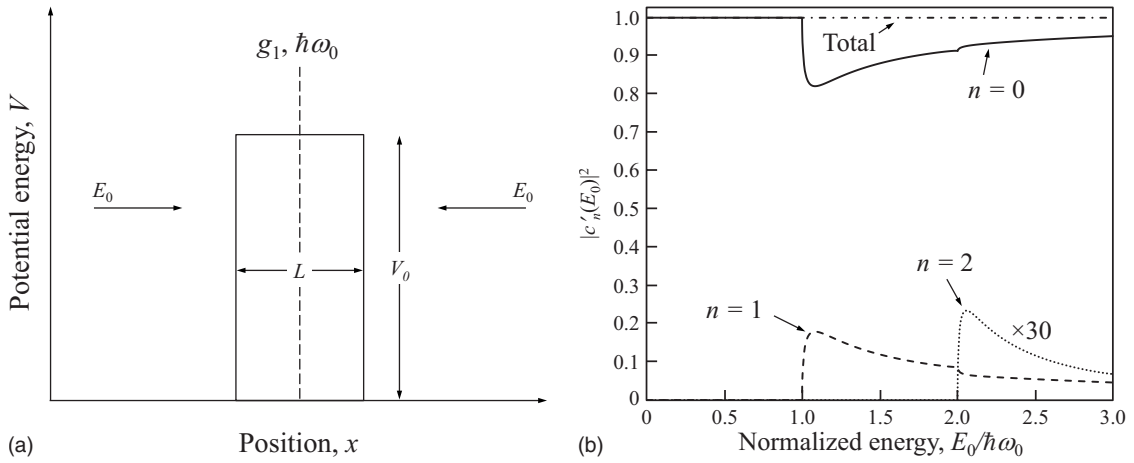

FIG. 2. (a) A rectangular potential barrier containing Einstein phonons (dotted line). The phonons are centered within the barrier and the electron injected with energy E_0 has plane-wave components incident from $\pm\infty$. (b) Probability of an electron of energy E_0 exiting the right-hand side of (a) in channel n. The potential barrier has energy $V_0=0.1$ eV and length $L=1$ nm, the phonons have energy $\hbar\omega_0=36$ meV, and the coupling constant is $g_1=0.05$ eV nm. The effective electron mass is $m=0.07m_0$, the number of inelastic channels included in the simulation is $N=11$, and the simulation converged with a relative error of less than 10^{-10}.

$$\cfrac{}{1-\cfrac{p^2}{1-\cfrac{p^2}{1-\cfrac{p^2}{\ddots}}}}, \tag{13}$$

where p is equal to Eq. (12). This is the continued fraction solution of the quadratic equation

$$x^2 - x + p^2 = 0 \Rightarrow x = 1 - \frac{p^2}{x}, \tag{14}$$

which diverges by oscillation if $1-4p^2<0$. Hence, from Eq. (12) one obtains $g_{1,c}=0.14$ eV nm for GaAs.

B. Simple first-order perturbation theory

Simple first-order perturbation theory predictions are obtained by truncating the continued fraction expansion solution at the first term in the Born series. This is equivalent to removing the first term from Eqs. (7) and (8) and only considering excitation of the first phonon. As an example, consider an electron of energy E_0 incident on Einstein phonons in an otherwise constant background potential $V(x)=0$ eV. The first-order perturbation theory solution of the transmitted waves is

$$c_0 = 1, \quad c_1 = -i\frac{mg_1}{\hbar^2 k_1}, \tag{15}$$

yielding a transmission of

$$T(E_0) = 1 + \frac{m^2 g_1^2}{\hbar^4 k_0 k_1}\theta(E_0 - \hbar\omega_0). \tag{16}$$

These results are clearly not self-consistent as the transmission violates unitarity and c_1 is infinite at $E_0=\hbar\omega_0$.

For comparison, the exact quantum solution considering only the $n=0$ and $n=1$ channels is

$$c_0 = \frac{1}{1+\dfrac{m^2 g_1^2}{\hbar^4 k_0 k_1}}, \quad c_1 = -i\frac{\dfrac{mg_1}{\hbar^2 k_1}}{1+\dfrac{m^2 g_1^2}{\hbar^4 k_0 k_1}}. \tag{17}$$

Simple first-order perturbation theory is usually justified on the basis of weak coupling, suggesting the g_1^2 term in the denominator can be ignored. However, it is this term that provides feedback between the channels and preserves unitarity, giving rise to important features in the quantum solution.

We compare the quantum and perturbative transmission spectra when the value of the coupling constant yields a matrix element equal to that of the Frölich interaction. The matrix element coupling initial state $|k_0\rangle$ to final state $|k_1\rangle$ is

$$|\langle k_1|\hat{H}|k_0\rangle|^2 = g_1^2|\psi_1(0)|^4. \tag{18}$$

For a conduction-band electron of energy $E_0=52$ meV interacting with an LO phonon in GaAs, Eq. (18) is equal to the matrix element for the Frölich interaction per unit volume when $g_1=0.008$ eV nm.

III. COMPARISON BETWEEN FIRST-ORDER PERTURBATION THEORY PREDICTIONS AND EXACT QUANTUM SOLUTION

A. Introduction to exact quantum solution

To understand the behavior of our model we first consider the system under symmetric conditions. For illustrative purposes, a unit amplitude sinusoidal wave function is injected from both the left- and right-hand sides of the spatially symmetric potential illustrated in Fig. 2(a). The probability of an electron of energy E_0 exiting the right-hand side of Fig. 2(a) in channel n is

$$|c_n'(E_0)|^2 = \frac{k_n}{k_0}|c_n(E_0)|^2. \tag{19}$$

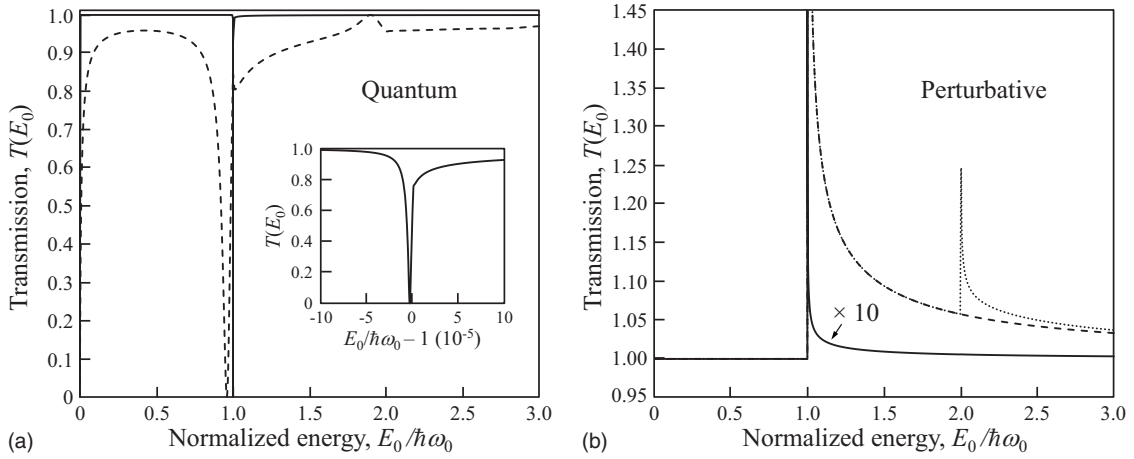

FIG. 3. Transmission through Einstein phonons located in a constant background potential $V(x)=0$ eV with coupling constants of $g_1=0.008$ eV nm (solid line) and $g_1=0.08$ eV nm (dashed line) using the (a) exact quantum solution and (b) perturbative solution including the $n=2$ channel to same order (dots). The electron of effective mass $m=0.07m_0$ is injected from $x=-\infty$ with energy E_0, the phonon energy is $\hbar\omega_0=36$ meV, and $N=11$ inelastic channels were included in the simulation. The inset shows the features of the transmission about $E_0=\hbar\omega_0$ with a coupling constant of $g_1=0.008$ eV nm on a fine energy scale.

For energies $E_0<\hbar\omega_0$, only $|c_0'|^2$ is nonzero. Once the $n=1$ channels open, this probability must decrease to preserve unitarity when $|c_1'|^2$ becomes finite. To a lesser extent $|c_0'|^2$ is also increased by the feedback as the electron may emit a phonon, reflect off the step change in the potential barrier, and reabsorb the phonon at position $x=x_0$. As a result the $n=0$ channel may not be considered an elastic channel. One may see that the feedback between the channels driven by unitarity gives rise to features in the spectrum.

B. Inelastic scattering in an otherwise constant background potential

When calculating inelastic-scattering rates, it is commonly assumed that weak coupling leaves the incident wave unchanged by the inelastic-scattering event and that simple first-order perturbation theory is an accurate approximation. Figure 3 shows that this is not the case. We show in Fig. 3(a) the quantum and in Fig. 3(b) the perturbative predictions for the transmission of an electron of energy E_0 incident from $x=-\infty$. The Einstein phonons are in a constant background potential $V(x)=0$ eV with coupling constants of $g_1=0.008$ eV nm (solid line) and $g_1=0.08$ eV nm (dashed line). The inset of Fig. 3(a) shows the features of the quantum transmission given a coupling constant of $g_1=0.008$ eV nm on a fine energy scale. Although these features are resolved due to the assumed long lifetime of the electron states, we anticipate that energy broadening due to finite lifetime effects will not qualitatively alter the results.

Rather than a decrease in transmission near $E_0=\hbar\omega_0$ predicted in the quantum case, the perturbative solution violates unitarity and has lost the features found in the exact quantum solution. Even under conditions of weak coupling with $g_1=0.008$ eV nm, the quantum and perturbative solutions are

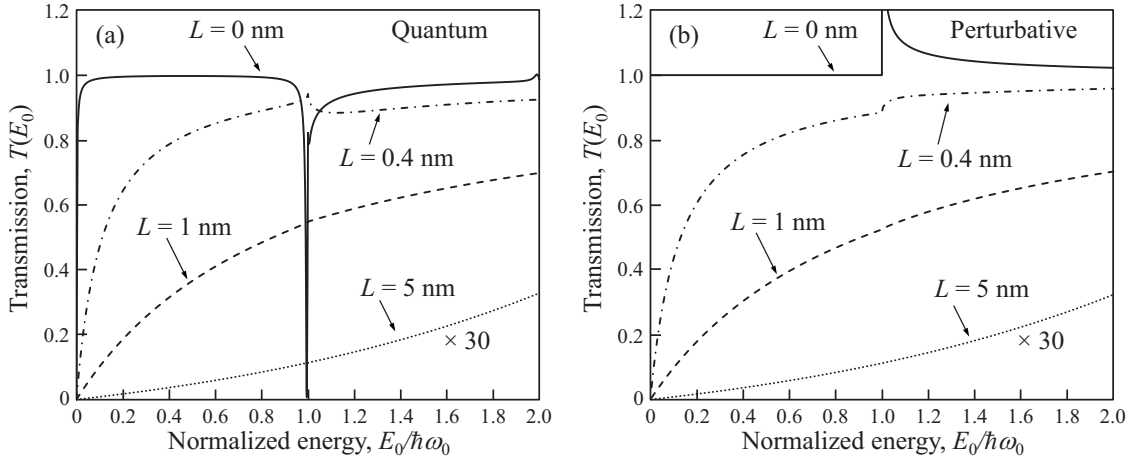

FIG. 4. (a) Quantum and (b) first-order perturbative solutions for the transmission of an electron of energy E_0 injected from $x=-\infty$ through the potential shown in Fig. 2(a). The potential barrier has energy $V_0=0.25$ eV and length L, $g_1=0.05$ eV nm, $\hbar\omega_0=36$ meV, the effective electron mass is $m=0.07m_0$, and $N=11$ inelastic channels were included in the simulation.

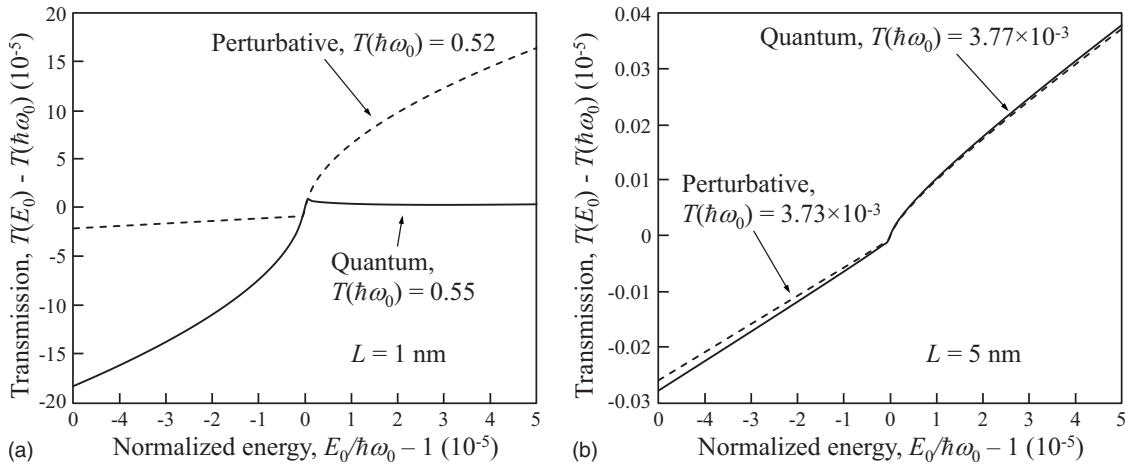

FIG. 5. Quantum (solid line) and perturbative (dashed line) transmissions from Fig. 4 shown on a fine scale for potential barrier lengths of (a) $L=1$ nm and (b) $L=5$ nm. The transmission curves have been offset by $T(\hbar\omega_0)$, so that the quantum and perturbative solutions may be compared. The potential barrier has energy $V_0=0.25$ eV and length L, and the phonon is characterized by $g_1=0.05$ eV nm and $\hbar\omega_0=36$ meV. $N=11$ inelastic channels were included in the simulation and the effective electron mass is $m=0.07m_0$.

dramatically different. Clearly weak coupling alone does not guarantee that the predictions of first-order perturbation theory will appear similar to the exact quantum solution.

C. Condition when perturbation solution appears similar to exact calculation

Consider the potential shown in Fig. 2(a) with an electron of energy E_0 injected from $x=-\infty$. The transmission through this system is shown for the quantum case in Fig. 4(a) and for the first-order perturbation theory approximation in Fig. 4(b). We use a rectangular potential barrier of energy $V_0=0.25$ eV and length L, and an electron-phonon coupling constant of $g_1=0.05$ eV nm. Again we use the relatively strong coupling constant to enhance the features.

For small L the features exhibited by the quantum and perturbative transmission spectra are dramatically different for energies both higher and lower than $E_0=\hbar\omega_0$. For lower energies the quantum transmission is influenced by the excitation of virtual phonons. Virtual phonon assisted tunneling increases the transmission probability by effectively lowering the energy of the potential barrier. This results in a higher transmission probability for the quantum transmission than the predictions of perturbative calculations. For energies greater than $E_0=\hbar\omega_0$, the $L=0.4$ nm perturbative transmission shows the semiclassical "opening of a new channel," whereas the quantum transmission does not. However, as L increases the transmission reduces and the quantum and perturbative solutions appear qualitatively similar on the scale shown.

Near $E_0=\hbar\omega_0$ the behavior of the two solutions become qualitatively similar for large L, as shown in Fig. 5. The figure shows the quantum (solid line) and perturbative (dashed line) solutions for the transmission shown in Fig. 4 for $L=1$ nm [Fig. 5(a)] and $L=5$ nm [Fig. 5(b)] on a fine energy and transmission scale. The transmission curves have been offset by $T(\hbar\omega_0)$, so that the two solutions may be compared.

For $L=5$ nm, the perturbative solution exhibits features qualitatively similar to those found in the quantum model. In both cases the transmission is well approximated by exponential tunneling through the barrier and a rapid increase occurs once the electron has enough energy to emit a phonon. However, the reflection spectra will not be qualitatively similar since the quantum reflection will reduce to preserve unitarity while the perturbative reflection will increase due to an additional channel for reflection. For the smaller barrier length, perturbation theory is not a good approximation to the quantum solution. Thus, as the strength of the potential barrier is increased the semiclassical transmission behavior predicted by first-order perturbation theory appears qualitatively similar to the behavior of the quantum model.

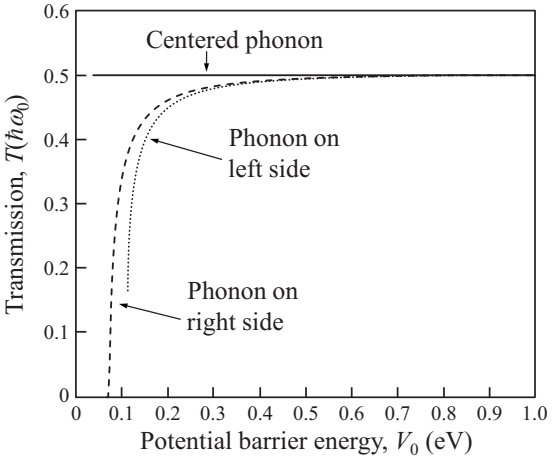

FIG. 6. Transmission coefficient at which $\partial T/\partial E_0=0$ at energy $E_0=\hbar\omega_0$ for three different phonon locations. In the simulation the potential barrier energy $V_0>\hbar\omega_0$ is fixed and the potential barrier length L is swept until $\partial T/\partial E_0=0$ at energy $E_0=\hbar\omega_0$. The simulation used a coupling constant of $g_1=0.008$ eV nm, phonon energy of $\hbar\omega_0=36$ meV, electron effective mass of $m=0.07m_0$, and $N=11$.

D. Threshold at which perturbation solution appears similar to exact calculation

We have seen that as the transmission coefficient decreases due to increasing potential barrier strength, the exact quantum transmission as a function of increasing electron energy changes from a decrease at the first phonon threshold to an increase. We choose

$$\left.\frac{\partial T}{\partial E_0}\right|_{E_0=\hbar\omega_0^+} = \left.\frac{\partial T_0}{\partial E_0}\right|_{E_0=\hbar\omega_0^+} + \left.\frac{\partial T_1}{\partial E_0}\right|_{E_0=\hbar\omega_0^+} \geq 0, \quad (20)$$

for the exact quantum case as the condition under which the features in the first-order perturbation theory solution appear qualitatively similar to those of the exact quantum solution. We consider the potential used in Fig. 4, and to simplify the expressions we consider only the $n=0$ and $n=1$ channels.

Evaluating the derivatives in Eq. (20) we find that

$$\left.\frac{\partial T_0}{\partial E_0}\right|_{E_0=\hbar\omega_0^+} = -T(\hbar\omega_0)\left(\left.\frac{\partial T_1}{\partial E_0}\right|_{E_0=\hbar\omega_0^+} + \left.\frac{\partial R_1}{\partial E_0}\right|_{E_0=\hbar\omega_0^+}\right)$$

$$= -2T(\hbar\omega_0)\left.\frac{\partial T_1}{\partial E_0}\right|_{E_0=\hbar\omega_0^+}, \quad (21)$$

where R_1 is the reflection coefficient of the $n=1$ channel and the last step comes from the spatial symmetry forcing T_1 and R_1 to be equal. Since the sum of the derivatives gives the total rate of change of the $n=1$ channel, the transmission coefficient is the fraction of this rate of change that is due to the transmission coefficient. The remaining fraction comes from the reflection coefficient. Substituting into Eq. (20), the features in the first-order perturbation theory solution appear similar to those of the quantum solution when

$$T(\hbar\omega_0) \leq \frac{1}{2}. \quad (22)$$

We see that similarity between the quantum and perturbative transmission spectra occurs when the transmission coefficient has reduced enough for a majority of the quantum feedback effects to occur in the reflection. If $T(\hbar\omega_0)$ is very small due to a large potential barrier, the transmission contributes little to the opening of the new inelastic channel and the simple first-order perturbation approximation emulates quantum behavior. The coupling constant contributes to this condition through the virtual phonon assisted tunneling. Larger coupling results in larger $T(\hbar\omega_0)$, which will require a stronger potential barrier to reach $T(\hbar\omega_0) \leq 1/2$.

If we move the phonon to one side of the potential barrier, the existence of a propagating state next to the phonon will enhance the inelastic scattering, while the reflection of only one inelastically scattered wave inside the barrier decreases the feedback. These two effects combine to make the transmission decrease faster at the phonon threshold, requiring a smaller transmission coefficient to reduce $\partial T_0/\partial E_0$ sufficiently that $\partial T/\partial E_0 > 0$. The condition becomes

$$T(\hbar\omega_0) \leq \frac{\cosh^2(\kappa_V L)}{2\left[\cosh^2(\kappa_V L) - \frac{1}{2}\sinh^2(\kappa_V L)\right]\left[\cosh^2(\kappa_\omega L) - \frac{1}{2}\left(1 - \frac{\hbar\omega_0}{V-\hbar\omega_0}\right)\sinh^2(\kappa_\omega L)\right]}, \quad (23)$$

when the phonon is located on the right side of the barrier, and

$$T(\hbar\omega_0) \leq \frac{\cosh^2(\kappa_\omega L) + \frac{\hbar\omega_0}{V-\hbar\omega_0}\sinh^2(\kappa_\omega L)}{2\left[\cosh^2(\kappa_V L) - \frac{1}{2}\sinh^2(\kappa_V L)\right]\left[\cosh^2(\kappa_\omega L) - \frac{1}{2}\left(1 - \frac{\hbar\omega_0}{V-\hbar\omega_0}\right)\sinh^2(\kappa_\omega L)\right]}, \quad (24)$$

when the phonon is located on the left side of the barrier, where $\kappa_V = \sqrt{2mV}/\hbar$ and $\kappa_\omega = \sqrt{2m(V-\hbar\omega_0)}/\hbar$.

We show in Fig. 6 the simulated transmission coefficient at which $\partial T/\partial E_0 = 0$ at energy $E_0 = \hbar\omega_0$ when the phonon is centered (solid line), placed on the right side (dashed line), and placed on the left side (dotted line) of the potential barrier. In the simulations, V_0 is fixed while L is swept until the condition is satisfied, with $g_1 = 0.008$ eV nm and $N=11$. Potential barrier lengths of up to $L=55$ nm were considered. As predicted the threshold occurs at $T(\hbar\omega_0) = 1/2$ when the phonon is centered independent of the strength of the potential barrier and smaller transmission coefficients are required for the asymmetric cases. However, as V_0 is increased L is decreased to achieve the threshold transmission, lessening the asymmetry and causing the three cases to converge as $L \to 0$.

When the phonon is placed on the left-hand side of the potential barrier the transmitted waves for both the $n=0$ and $n=1$ channels must tunnel through the potential barrier before exiting the system. The $n=1$ channel has a larger decay constant than the $n=0$ channel, decreasing T_1 more than T_0 and requiring a smaller $\partial T_0/\partial E_0$ to satisfy Eq. (20). For potential barrier energy on the order of the phonon energy this effect becomes so great that first-order perturbation theory does not approximate well the quantum solution for any barrier length L. In Fig. 6 the cutoff occurs at $V_0 = 111.4$ meV

and $L=4$ nm. One may make the argument that requiring the transmission coefficient to be small in order for perturbation theory to be a good approximation is equivalent to requiring the inelastic coupling strength be weak relative to the elastic-scattering strength. However, the existence of the cutoff shows that this is not the case as the combination of weak coupling and large elastic-scattering strength is not always sufficient. Thus, even in the case of weak coupling and large potential barrier length, conditions exist under which perturbation theory cannot appear qualitatively similar to the exact quantum solution.

IV. CONCLUSION

We have shown that weak coupling alone is not a sufficient condition for the predictions of simple first-order perturbation theory to qualitatively approximate the nonperturbative quantum predictions of electron transmission spectra in the presence of electron-phonon interaction. Only if the transmission coefficient is small enough at the phonon threshold, causing the feedback effects to occur primarily in reflection, can the quantum and perturbative solutions appear qualitatively similar. The conditions under which this similarity can occur are determined analytically. There are situations in which predictions of perturbation theory cannot approach the quantum calculation even in the presence of both weak coupling and large elastic-scattering strengths. Calculation of inelastic electron transmission using simple first-order perturbation theory is a fundamentally flawed approach for a unitary system. Qualitative agreement with nonperturbative calculation of inelastic electron transmission spectra occurs only under highly restrictive conditions.

*magruder@usc.edu

[1] Y. Meir and N. S. Wingreen, Phys. Rev. Lett. **68**, 2512 (1992).
[2] R. Landauer, IBM J. Res. Dev. **1**, 223 (1957).
[3] R. Landauer, Philos. Mag. **21**, 863 (1970).
[4] B. Y. Gelfand, S. Schmitt-Rink, and A. F. J. Levi, Phys. Rev. Lett. **62**, 1683 (1989).
[5] J. Bonča and S. A. Trugman, Phys. Rev. Lett. **75**, 2566 (1995).
[6] K. Haule and J. Bonča, Phys. Rev. B **59**, 13087 (1999).
[7] E. G. Emberly and G. Kirczenow, Phys. Rev. B **61**, 5740 (2000).
[8] T. Brandes and J. Robinson, Phys. Status Solidi B **234**, 378 (2002).
[9] B. P. W. de Oliveira and S. Haas, Phys. Rev. B **79**, 155102 (2009).
[10] S. Monturet and N. Lorente, Phys. Rev. B **78**, 035445 (2008).
[11] W. Lee, N. Jean, and S. Sanvito, Phys. Rev. B **79**, 085120 (2009).
[12] E. O. Kane, in *Tunneling Phenomena in Solids*, edited by E. Burstein and S. Lundqvist (Plenum Press, New York, 1969), pp. 1–11.
[13] A. F. J. Levi, *Applied Quantum Mechanics* (Cambridge University Press, Cambridge, UK, 2006), pp. 171–181.